Progress In Electromagnetics Research, PIER 92, 195–208, 2009

A DUAL-BAND CIRCULARLY POLARIZED STUB LOADED MICROSTRIP PATCH ANTENNA FOR GPS APPLICATIONS

A. A. Heidari, M. Heyrani, and M. Nakhkash

Department of Electrical Engineering
Yazd University
P. O. Box 89195-741, Yazd, Iran

Abstract—A single-feed low-profile and easy to fabricate circularly polarized microstrip patch antenna has been developed for GPS applications. For dual frequency operation, four slots are etched near edges of the patch and a crossed slot etched in the center for generating circular polarization. In order to reducing the frequency ratio of two frequency bands of the antenna, the patch is loaded by four short circuit microstrip stubs. The paper reports several simulation results that confirm the desired characteristics of the antenna. Using stub loading, the frequency ratio of two bands of the antenna can be, even, reduced to 1.1.

1. INTRODUCTION

Most current global positioning system (GPS) receivers only operate at L_1 frequency of 1575 MHz with right hand circular polarization (CP). Requiring more accurate information, some applications employ differential GPS whose antenna covers both L_1 and L_2 (1227 MHz) bands. The antenna of a special GPS transmitter (e.g., GPS jammer) is, also, required to cover the two bands. Considering the GPS signals occupy the bandwidth of about 20 MHz, another requirement is to design antennas with minimum 20 MHz bandwidth in either L_1 or L_2 band.

The GPS antennas can be implemented in many different types, such as the quadra-filar spiral [1]. Nevertheless, the first consideration over other conventional antennas would be microstrip antennas due to being lightweight, low-profile, low-cost and possessing other remarkable

Corresponding author: A. A. Heidari (aheidari@yazduni.ac.ir).

advantages. The major limitation of microstrip antennas is their narrow bandwidth. Although different techniques are proposed [2, 3] to increase the bandwidth, practical implementation of many of these structures involves complex process that makes them uneconomical for mass production. Furthermore, a broadband antenna whose frequency width extends from L_1 to L_2 receives noise and parasite through the undesired frequency range. Narrow bandwidth of microstrip patch antennas makes researchers think of dual-band antennas.

Various patch antenna structures have been reported for dual-band operation with circular polarization [4–11] and specially for GPS applications [4, 5, 8–11]. The proposed antenna in [4] is a circularly polarized stacked patch antenna with aperture coupling feed. Fabrication of this antenna is not cost effective, because of its multilayer structure and its feeding network. A single-layer dual-band microstrip antenna for GPS applications is reported in [5], in which the antenna has four switches on four slots on the path. This antenna needs a control circuit for switches and has another problem that cannot operate in both frequency bands simultaneously. The antenna configuration in [6] needs two perpendicular ports and two power dividers to provide 90° phase shift for each band. Therefore, it cannot operate in both frequency bands simultaneously.

In [7], a single-feed slotted patch antenna is proposed for generating circular polarization in two frequency bands. For such a dual-frequency design, the frequency ratio of two operating frequencies is generally within the range [1.5, 2] when a suitable slot length is chosen; but GPS applications need an antenna with frequency ratio about 1.28. To overcome this limitation, recently a dual band CP microstrip antenna for GPS application has been proposed [9]. This antenna produce circular polarization without a cross slot in the center of the patch. A dual-band antenna structure was proposed in [12] that the frequency ratio of two operating bands can be in the range of 1.04 to 1.4, but it is not a CP antenna.

This paper introduces a square microstrip patch antenna that achieves dual-band CP radiation for GPS applications. The novel idea employed in this paper is to use a single-feed slotted patch structure and load it reactively so as to reduce the frequency ratio of two bands. This together with single-probe feeding makes the antenna a cost effective choice for mass production. Simulation results were obtained using the HFSS software. The paper reports several simulation results that confirm the desired characteristics of the antenna.

2. ANTENNA DESIGN

The most important parameter in our designing process is the simplicity of the antenna and its feeding structure so that the antenna can be fabricated easily in practice. Therefore, slot loaded patch antenna with a coaxial feed was considered as a base structure.

2.1. Basic Antenna Structure

Dual frequency operation of the slot loaded patch antenna was investigated in [13]. When two narrow slots are etched close to the radiating edges, the TM_{100} mode is perturbed a little, whereas significant perturbation occurs for TM_{300} mode. Because perturbed TM_{300} mode has a radiation pattern similar to that of TM_{100} mode, the excitement of the two modes results in the dual band operation of the antenna.

Figure 1 shows the basic structure of a dual band slotted patch antenna. For producing circular polarization, the square patch must have four slots at the edges and a cross slot at the center. Without cross slot, the structure in Figure 1 has a 45° linear polarization. The cross slot excites two orthogonal modes with equal amplitude but 90° out of phase, yielding CP radiation. An air layer (foam) is also used for increasing the impedance band-width of the antenna. Such a structure generally provides a frequency ratio within interval [1.5, 2] for the two operating frequencies. Therefore, reduction in the frequency ratio is required for GPS application.

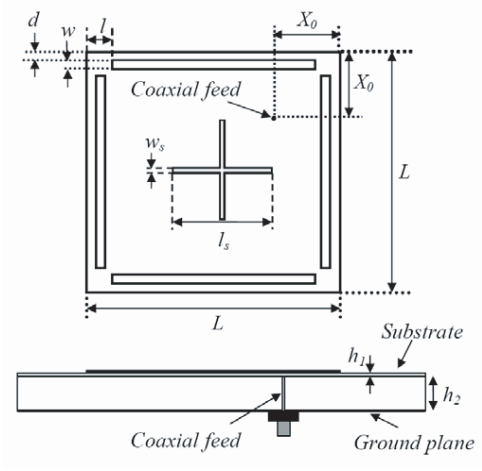

Figure 1. A dual band coaxial feed slotted antenna.

2.2. Reactive Loading the Antenna

Among the methods used to change the resonance frequency of a patch antenna is to load it with a reactive element [14, 15]. Figure 2 shows a simple circuit model for the input impedance of reactively loaded patch antenna. Using this model, the characteristic equation for estimating the new resonance frequency is:

$$X_r = -\left(X_f + X_L/(1+\alpha)\right) \tag{1}$$

where X_r is the unloaded patch reactance, X_f is the feed reactance, X_L is the load reactance and α is a constant [14, 15]. In order to develop important design concepts, it is useful to solve Equation (1) graphically. Such a graphical solution is illustrated in Figure 3, where the right and left sides of Equation (1) is plotted for an inductive load. The intersection point of two curves is the new resonance frequency. If the effect of X_f is neglected, two consequences can be drawn from the figure: 1 — If the load is inductive, the resonance frequency increases and if the load is capacitive, the resonance frequency decreases. 2 —

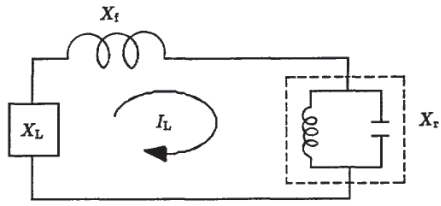

Figure 2. Circuit model for the input impedance of reactively loaded patch antenna [14].

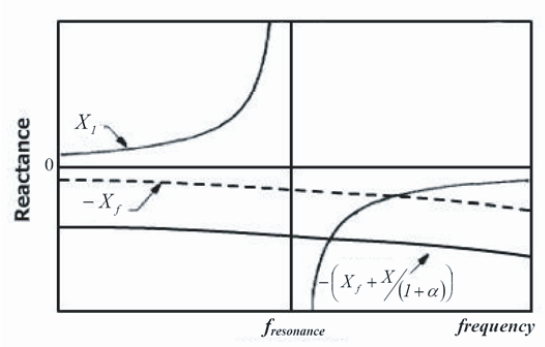

Figure 3. Plot of the left and right sides of Equation (1) for inductive load.

As much as the reactive load is smaller, the frequency shift is wider, i.e., the frequency shift may be written as

$$\left| f' - f \right| \propto \frac{1}{X_L} \tag{2}$$

According to the above discussion, in order to shift the frequency bands of the antenna and reduce the frequency ratio, the slotted patch antenna is loaded symmetrically by four short or open circuit microstrip stubs. Figure 4 shows the modified structure with short circuit stubs, which are "L" shape to reduce the size of the antenna. The length l_1 should be so long that the stubs do not affect the radiation pattern of the antenna. The stub length $l_1 + l_2$ is determined such that the input impedance of the lines is inductive in the lower band and capacitive in the higher band. In this way, the frequency ratio is reduced since the lower resonance frequency, f_1, increases and the higher resonance frequency, f_2, decreases.

The proper length of the stubs is calculated with respect to the input impedance of a short circuit stub [16]:

$$Z_{in} = jZ_0 \tan\left(\frac{2\pi l_{stub}}{\lambda}\right) \tag{3}$$

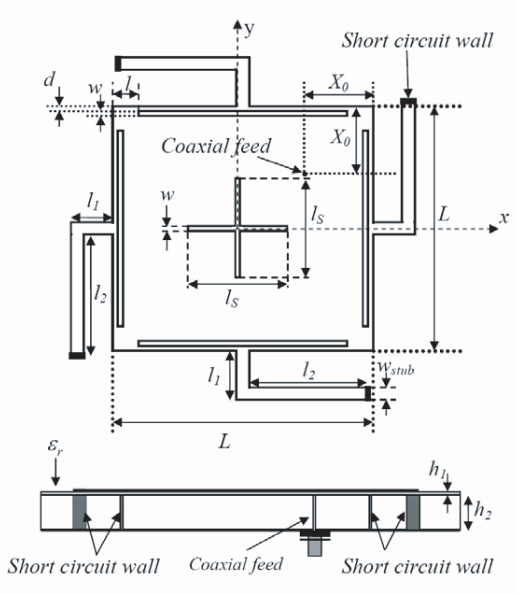

Figure 4. Top and side view of the proposed antenna structure.

where Z_0 is the characteristic impedance of the line, $l_{stub} = l_1 + l_2$ is the stub length and λ denotes the wavelength in the stub. The input impedance needs to be capacitive at higher frequency f_2 (i.e., when the reactance becomes negative). Thus, we have

$$X_{in} < 0 \Rightarrow \tan\left(\frac{2\pi l_{stub}}{\lambda_2}\right) < 0$$

that results in

$$\frac{\lambda_2}{4} < l_{stub} < \frac{\lambda_2}{2} \quad \text{or} \quad \frac{3\lambda_2}{4} < l_{stub} < \lambda_2 \tag{4}$$

Similarly the input impedance becomes inductive at f_1 if

$$X_{in} > 0 \Rightarrow \tan\left(\frac{2\pi l_{stub}}{\lambda_1}\right) > 0$$

concluding in

$$l_{stub} < \frac{\lambda_1}{4} \quad \text{or} \quad \frac{\lambda_1}{2} < l_{stub} < \frac{3\lambda_1}{4} \tag{5}$$

The stub length needs to satisfy the conditions in (4) and (5) simultaneously and therefore

$$\frac{\lambda_2}{4} < l_{stub} < \frac{\lambda_1}{4} \tag{6}$$

If open circuit stub is used, similar analysis shows that the stub length must satisfy the condition

$$\frac{\lambda_2}{2} < l_{stub} < \frac{\lambda_1}{2} \tag{7}$$

Comparing (6) and (7), the use of the short circuit stub reduces the stub length and overall antenna size. If the antenna size is not a critical factor, using open circuit stubs can simplify the fabrication process.

3. SIMULATION RESULTS AND DISCUSSION

3.1. Verifying Stub Effects

It is instructive to verify the effects of the stub parameters on the frequency ratio of two resonance frequencies of the antenna. Before designing the complete antenna structure in Figure 4, we investigate

the characteristics of the antenna structure in Figure 1 without the center cross slot. Using approximate design formulas in [13], the parameters in Figure 1 are set to: $L = 100\,\text{mm}$, $X_0 = 40\,\text{mm}$, $w = 2\,\text{mm}$, $d = 2\,\text{mm}$, $l = 10\,\text{mm}$, $h_1 = 0.6\,\text{mm}$, $h_2 = 5\,\text{mm}$ and the dielectric constant of substrate $\varepsilon_r = 2.2$. Simulation result for the return loss of the antenna is shown in Figure 5, where it can be observed the antenna resonates at two frequencies of $f_1 = 1.19\,\text{GHz}$ and $f_2 = 1.65\,\text{GHz}$. This gives the frequency ratio of about 1.39 that should be decreased for our application.

For decreasing this frequency ratio, the antenna is loaded by microstrip stubs as in Figure 4. Using relation (6), the length of the stubs can be in the range: $45.5\,\text{mm} < l_{stub} < 63\,\text{mm}$ with the assumption that $\varepsilon_{reff} \cong 1$. After adding the stubs to the previous structure, the antenna is simulated for various stub lengths within the above range and the resultant return losses are shown in Figure 6. This figure reveals that the frequency ratio is reduced by increasing the lower resonance frequencies and decreasing the higher ones. It is interesting to note that for the $l_{stub} = 63\,\text{mm}$, the lower resonance frequency ($f_1 = 1.19\,\text{GHz}$) is nearly equal for loaded and unloaded cases. One could predict such a result because the stub length is equal to $\lambda_1/4$ in this frequency and the stubs behave like open circuit.

We carry out another simulation to confirm the validity of the model presented in Subsection 2.2. If the stub length is selected

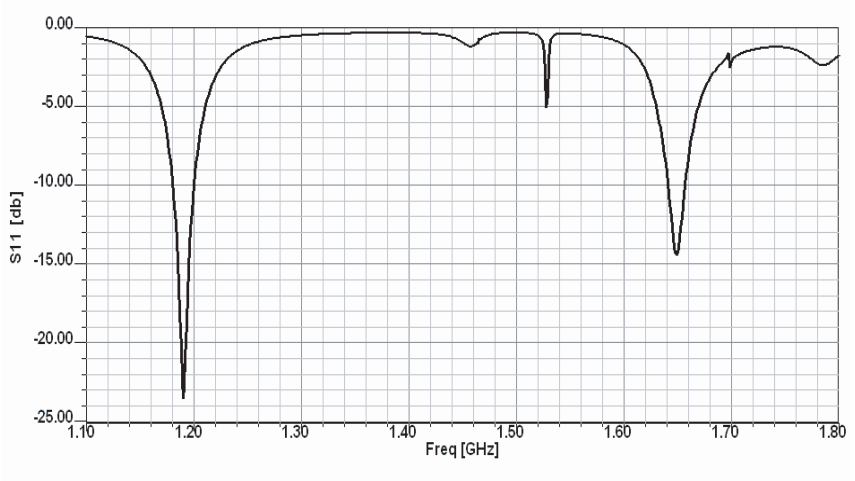

Figure 5. Return loss of the antenna in Figure 1 without the cross slot.

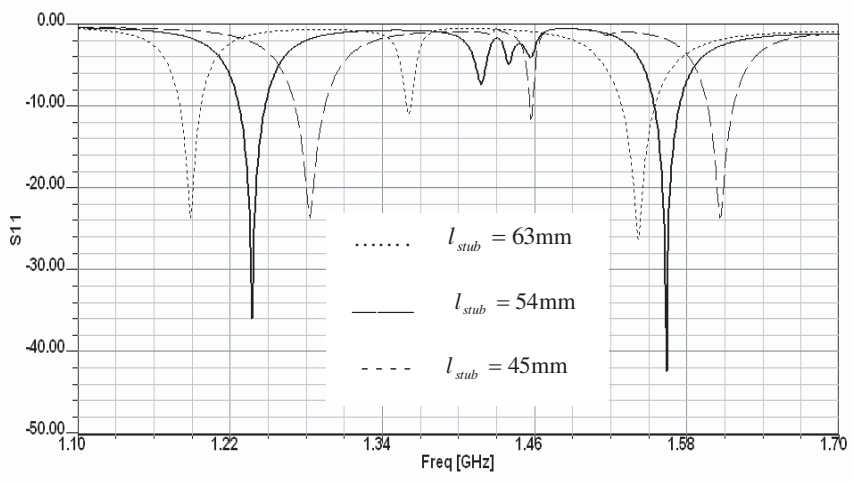

Figure 6. Return loss of the reactive loaded antenna for various stub lengths ($l_{stub} = l_1 + l_2$). The other parameters are as: $w_{stub} = 5\,\text{mm}$, $L = 100\,\text{mm}$, $X_0 = 40\,\text{mm}$, $w = 2\,\text{mm}$, $d = 2\,\text{mm}$, $l = 10\,\text{mm}$, $h_1 = 0.6\,\text{mm}$, $\varepsilon_r = 2.2$, $h_2 = 5\,\text{mm}$, $l_1 = 20\text{mm}$, $l_2 = l_{stub} - l_1$, $w_2 = 5\,\text{mm}$.

Table 1. Summary of the results presented in Figures 5–7.

Stub length (mm)	**Without stub**	**63**	**54**	**45**	**39**	**33**	**27**
f_1 **(MHz)**	1190	1190	1238	1283	1313	1344	1353
f_2 **(MHz)**	1650	1541	1565	1605	1660	1700	1760
f_1/f_2	1.386	1.295	1.264	1.252	1.264	1.265	1.3

smaller than the range of relation (6), i.e., $l_{stub} < \lambda_2/4$, the stub will be inductive and the model predicts the higher resonance frequency will be increased. Simulating the antenna for $l_{stub} < \lambda_2/4$, Figure 7 illustrates this prediction. So as to make a better comparison, Table 1 summarizes the aforementioned simulation results for the resonance frequencies of the antenna and the ratio of them. This table indicates the frequency ratio can be decreased from 1.39 to 1.25 by loading the antenna and decreasing the stub lengths.

The effect of the microstrip line's width on the antenna characteristics is also explored. As Figure 8 shows, the frequency ratio is decreased by widening the microstrip lines. This phenomenon can be explained noting that the characteristic impedance of the stubs and the

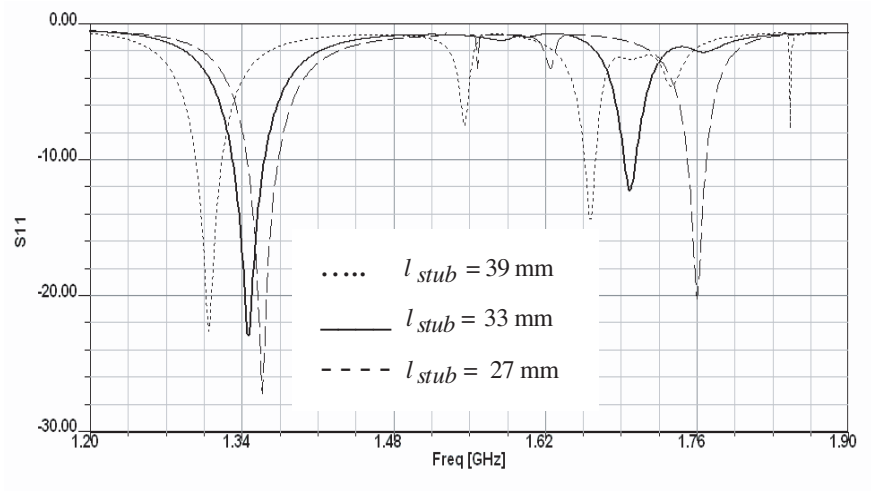

Figure 7. Return loss of the reactive loaded antenna for the case $l_{stub} < \lambda_2/4$. The other parameters are as in Figure 6.

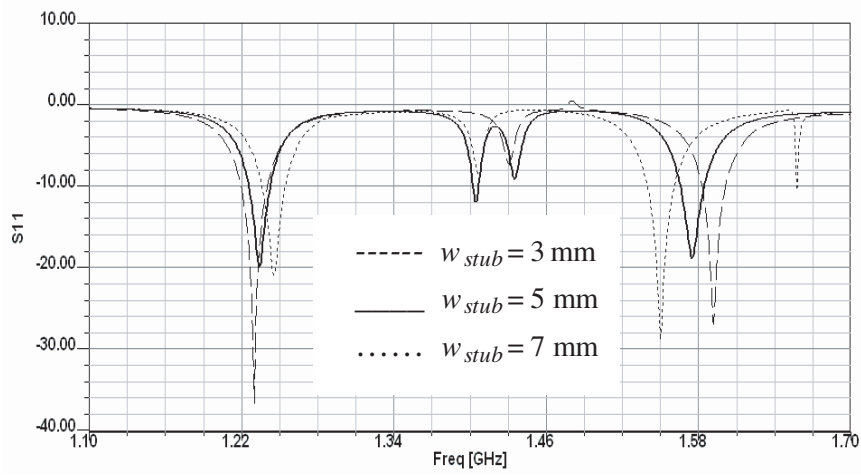

Figure 8. Return loss of the previous antenna for different microstrip lines width ($l_{stub} = 54$ mm).

input reactance of them is a decreasing function of the line's width. By the virtue of relation (2) and Figure 3, one can observe the frequency ratio will be decreased as the lines are widened.

3.2. Simulating the Proposed Antenna

In the previous subsection, the stub properties were investigated for a dual-band linear polarized antenna (i.e., the structure of Figure 4 without cross slot). The inclusion of a cross slot at the center of the patch can modify the linear polarization to the right hand circular polarization. This modification requires the adjustment of the cross slot parameters and the coaxial feed position on diameter of the patch for exciting two orthogonal modes with equal amplitude but 90° out of phase. However, it should be noted that the variation of the cross slot parameters changes the resonance frequencies of the antenna, as well. In other words, there would be several parameters that should be tuned to achieve satisfactory performance. This proposes an optimization process for the antenna design in terms of several variables, which is a time consuming process.

Numerical simulation of the antenna using HFSS is a time consuming process and it is not easy to optimize several parameters of the antenna using conventional optimization algorithms. Hence the antenna was optimized using a manually procedure. The optimization involves an iterative process consisting of the antenna simulation for given parameters, evaluating the antenna performance and the change of the parameters in a guided manner according to the required characteristics. Without providing the results within the process, the final antenna has the following parameters (Figure 4):

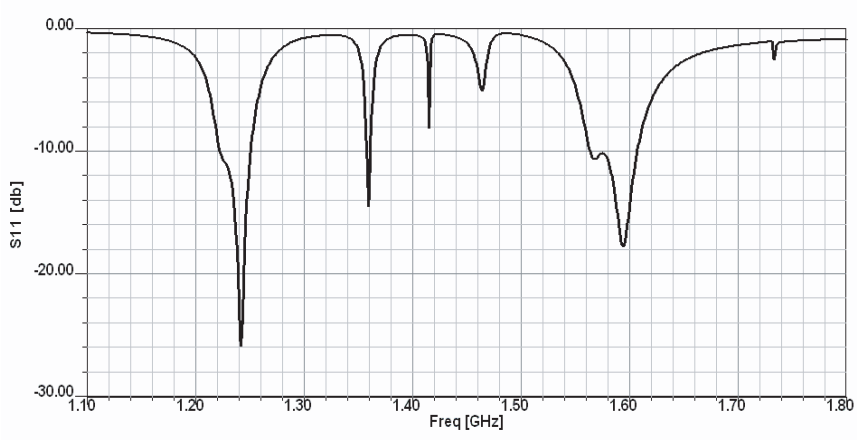

Figure 9. Return loss of the final proposed antenna.

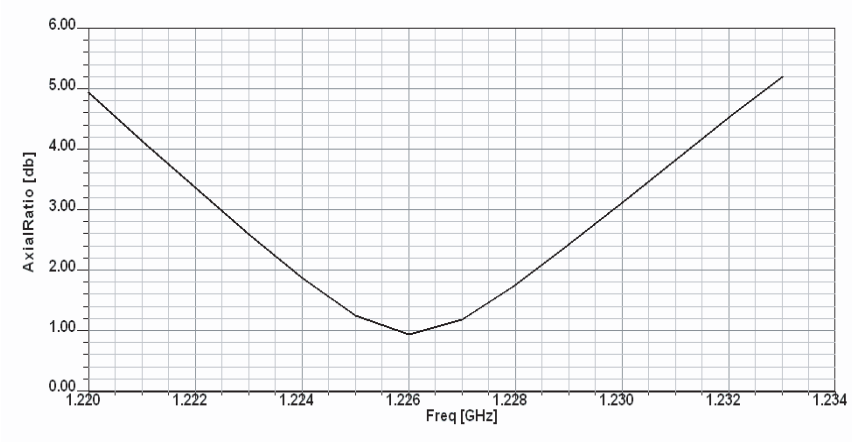

Figure 10. Axial ratio of the final proposed antenna in L_2 band.

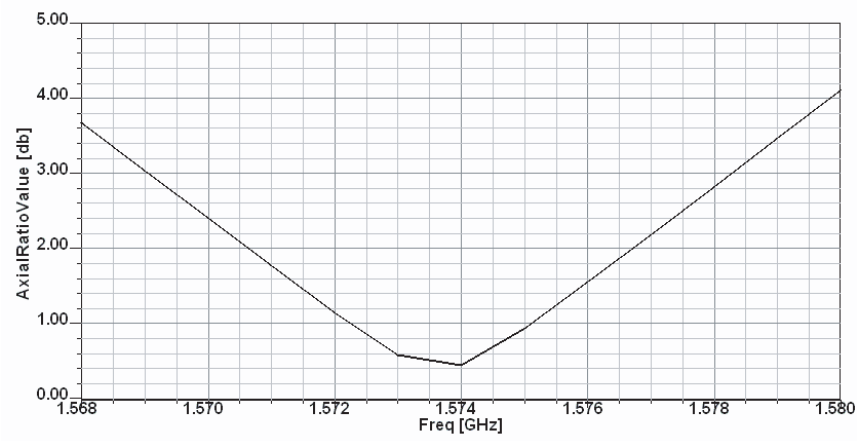

Figure 11. Axial ratio of the final proposed antenna in L_1 band.

$$
\begin{aligned}
L &= 99\,\text{mm}, \quad X_0 = 39\,\text{mm}, \quad w = 2\,\text{mm}, \quad d = 2\,\text{mm}, \\
l &= 10\,\text{mm}, h_1 = 0.6\,\text{mm}, \quad \varepsilon_r = 2.2, \quad h_2 = 5\,\text{mm}, \\
l_1 &= 20\,\text{mm}, \quad l_2 = 39, \quad w_2 = 5\,\text{mm}, \quad l_s = 33.6\,\text{mm}, \quad w_s = 2\,\text{mm}.
\end{aligned}
$$

The return loss of this antenna is shown in Figure 9, where it can be seen the impedance bandwidth in L_1 (1575 MHz) and L_2 (1227 MHz) are greater than the minimum required bandwidth (20 MHz) for GPS application. Extra run of the design process show that the frequency ratio of two bands of the antenna could reach 1.1 that can be employed for other applications. Axial ratio of the antenna is shown in Figures 10

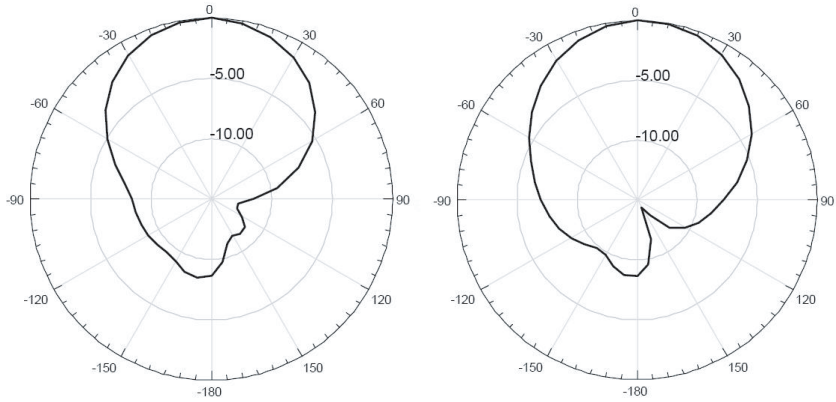

(a) *x*-*z* plane (b) *y*-*z* plane

Figure 12. Radiation patterns of the final proposed antenna at 1575 MHz.

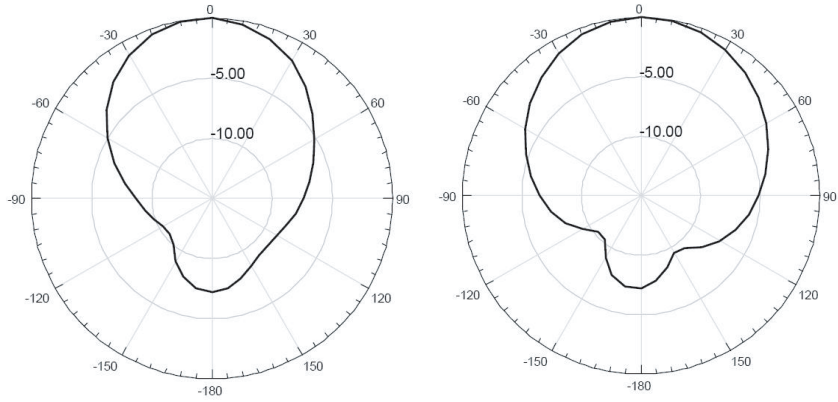

(a) *x*-*z* plane (b) *y*-*z* plane

Figure 13. Radiation patterns of the final proposed antenna at 1227 MHz.

and 11 for the two bands. One can see the axial ratio bandwidth is narrower than the impedance bandwidth, as this is usual for microstrip antennas. Figures 12 and 13 give the radiation pattern of the antenna at the L_1 and L_2 frequencies, illustrating the stubs have no destructive effect on the radiation pattern. Simulation results show that the gain of the antenna in the L_1 and L_2 bands are approximately 6.46 and 6.78 dB respectively. The antenna efficiency is about 98%.

4. CONCLUSION

This paper introduces a new antenna structure that is low-profile and low-cost for GPS (transmitter or receiver) applications. It, also, describes reactive loading technique using short circuit microstrip stubs to reduce the frequency ratio of a slotted patch dual-band antenna.

The simulation results show the existence of the stubs has no destructive effect on the radiation pattern. Optimizing the antenna, the frequency ratio of two bands of the antenna can, further, be reduced to 1.1.

ACKNOWLEDGMENT

This work was supported financially by Iran Telecommunication Research Center (ITRC).

REFERENCES

1. Padros, N., J. Ortigosa, J. Baker, M. Iskander, and B. Thomberg, "Comparative study of high-performance GPS receiving antenna design," *IEEE Trans. Antennas Propagat.*, Vol. 45, No. 4, 698–706, 1997.
2. Garg, R., P. Bhartia, I. Bahl, and A. Ittipiboon, *Microstrip Antenna Design Handbook*, Artech House Inc., 2001.
3. Sanchez-Hernandez, D. and I. D. Robertson, "A survey of broadband microstrip patch antennas," *Microwave J.*, 60–84, Sep. 1996.
4. Pozar, D. M. and S. M. Duffy, "A dual-band circularly polarized aperture-coupled stacked microstrip antenna for global positioning satellite," *IEEE Trans. Antennas Propagat.*, Vol. 45, No. 11, 1618–1624, Nov. 1997.
5. Yang, F. and Y. Rahmat-samii, "A single layer dual band circularly polarized microstrip antenna for GPS applications," *IEEE Antennas Propagat. Society International Symposium*, Vol. 4, 720–723, 2002.
6. Yu, A., F. Yang, and A. Elsherbeni, "A dual band circularly polarized ring antenna based on composite right and left handed metamaterials," *Progress In Electromagnetics Research*, PIER 78, 73–81, 2008.
7. Yang, K. P. and K. L. Wong, "Dual band circularly polarized square microstrip antenna," *IEEE Trans. Antennas Propagat.*, Vol. 49, No. 3, 378–382, March 2001.

8. Lan, X., "A novel high performance GPS microstrip antenna," *IEEE Antennas and Propagat Society International Symposium*, Vol. 2, 988–991, 2000.
9. Fujimoto, T., D. Ayukawa, K. Iwanaga, and M. Taguchi, "Dual-band circularly polarized microstrip antenna for GPS applications," *IEEE Antennas and Propagat Society International Symposium AP-S 2008*, 1–4, 2008.
10. Sim, C.-Y.-D., "A single layer dual-band CP microstrip antenna for GPS and DSRC applications," *Journal of Electromagnetic Waves and Applications*, Vol. 22, 529–539, 2008.
11. Chou, H.-T., L.-R. Kuo, and W.-J. Liao, "Characteristic evaluation of an active patch antenna structure with an embedded LNA module for GPS reception," *Journal of Electromagnetic Waves and Applications*, Vol. 21, No. 5, 599–614, 2007.
12. Alkanhal, M. A. and A. F. Sheta, "A novel dual-band reconfigurable square-ring microstrip antenna," *Progress In Electromagnetics Research*, PIER 70, 337–349, 2007.
13. Maci, S., G. B. Gentili, P. Piazzesi, and C. Salvador, "Dual-band slot-loaded patch antenna," *IEE Proceedings Microwave Antennas and Propagat.*, Vol. 142, No. 3, 225–232, June 1995.
14. Richards, W. F. and S. A. Long, "Reactively loaded microstrip antennas," *IEEE Antennas and Propagat Society Newsletter,* Vol. 28, No. 5, 10–17, Oct. 1986.
15. Richards, W. F., S. E. Davidson, and S. A. Long, "Dual-band reactively loaded microstrip antenna," *IEEE Trans. Antennas Propagat.*, Vol. 33, No. 5, 556–561, May 1985.
16. Pozar, D. M., *Microwave Engineering*, 3rd edition, John Wiley and Sons Inc., 2004.